Received 7 June 2020; revised 2 July 2020; accepted 10 July 2020. Date of publication 13 July 2020; date of current version 28 July 2020.

Digital Object Identifier 10.1109/OJCOMS.2020.3009023

Enabling Remote Human-to-Machine Applications With AI-Enhanced Servers Over Access Networks

SOURAV MONDAL [1] (Graduate Student Member, IEEE), LIHUA RUAN [1] (Member, IEEE), MARTIN MAIER [2] (Senior Member, IEEE), DAVID LARRABEITI [3] (Senior Member, IEEE), GOUTAM DAS [4] (Member, IEEE), AND ELAINE WONG [1] (Senior Member, IEEE)

[1]Department of Electrical and Electronic Engineering, University of Melbourne, Melbourne, VIC 3010, Australia

[2]Optical Zeitgeist Laboratory, INRS, Montréal, QC H5A 1K6, Canada

[3]Telematics Engineering Department, Charles III University of Madrid, 28911 Madrid, Spain

[4]G. S. Sanyal School of Telecommunications, Indian Institute of Technology Kharagpur, Kharagpur 721302, India

CORRESPONDING AUTHOR: S. MONDAL (e-mail: smondal@student.unimelb.edu.au)

This work was supported by the John Collier Scholarship from Melbourne School of Engineering in 2019 to support research students to undertake valuable travel opportunities.

ABSTRACT The recent research trends for achieving ultra-reliable and low-latency communication networks are largely driven by smart manufacturing and industrial Internet-of-Things applications. Such applications are being realized through Tactile Internet that allows users to control remote things and involve the bidirectional transmission of video, audio, and haptic data. However, the end-to-end propagation latency presents a stubborn bottleneck, which can be alleviated by using various artificial intelligence-based application layer and network layer prediction algorithms, e.g., forecasting and preempting haptic feedback transmission. In this paper, we study the experimental data on traffic characteristics of control signals and haptic feedback samples obtained through virtual reality-based human-to-machine teleoperation. Moreover, we propose the installation of edge-intelligence servers between master and slave devices to implement the preemption of haptic feedback from control signals. Harnessing virtual reality-based teleoperation experiments, we further propose a two-stage artificial intelligence-based module for forecasting haptic feedback samples. The first-stage unit is a supervised binary classifier that detects if haptic sample forecasting is necessary and the second-stage unit is a reinforcement learning unit that ensures haptic feedback samples are forecasted accurately when different types of material are present. Furthermore, by evaluating analytical expressions, we show the feasibility of deploying remote human-to-machine teleoperation over fiber backhaul by using our proposed artificial intelligence-based module, even under heavy traffic intensity.

INDEX TERMS Human-to-machine applications, reinforcement learning, supervised learning, ultra-low latency communication.

I. INTRODUCTION

THE TACTILE Internet (TI) envisions a telecommunication network that supports and empowers human users to immersively control and manipulate both real and virtual remote things or machines [1]. Within the next few decades, the Internet-of-Things (IoT) will play an essential role in our daily lives as well as in industrial manufacturing (Industry 4.0). In this technical evolution process of IoT, enabling the interaction among machines and humans over the Internet appears as a fundamental requirement [2]. The IEEE P1918.1 standards working group defined TI as "A network (or network of networks) for remotely accessing, perceiving, manipulating, or controlling real or virtual objects or processes in perceived real-time by humans or machines" [3] and some primary use cases considered are teleoperation, immersive virtual/augmented reality (VR/AR),

and industrial automotive control [4]. The authors of [5] indicated that there is an overlap in the concepts and technologies related to IoT, 5G and TI, such as ultra-low-latency (1-10 ms) and high-reliability (99.999%) communication channels, high-bandwidth, and secure network infrastructure with integrated edge computing intelligence. Most of these applications involve remote immersion that is achieved through bilateral exchange of multi-modal information, e.g., a combination of audio, video, and haptic information over the Internet with reaction latencies of 100 ms, 10 ms, and 1 ms, respectively [1].

The term "haptics" refers to both "kinesthetic perception", i.e., forces, torques, position, and velocity experienced by the muscles, joints, and tendons of the body and "tactile perception", i.e., surface texture and friction sensed by different types of mechanoreceptors in the skin [6]. The latency requirements of haptic communications are dependent on the intensity of control dynamics involved in the application scenario. For applications with "low dynamics" like remote surgery and "intermediate dynamics" like a collaboration of users in virtual or real environments, it is possible to involve human users in a closed global control loop between the human users and the teleoperators, thus leading to human-to-machine (H2M) applications [7]. A typical H2M communication system consists of a "master subsystem" and a "slave subsystem" that interact over a network, as shown in Fig. 1. A human operator at the master subsystem end generates and transmits control signals, i.e., position and velocity data through motion sensors, over a communication channel. In return, the slave subsystem receives that data and responds back with force reflection/feedback of the remote environment, in the form of kinesthetic or vibrotactile force feedback data [8].

In order to maintain the system stability and transparency, haptic sensor readings from kinesthetic devices are typically sampled, packetized and transmitted at a rate of 1 kHz or higher [9]. The authors of [10]–[12] performed stability analyses to show that there is a relationship between the sampling rate, the overall stiffness shown, and the damping of the system to ensure system stability. An H2M system that operates with lower sampling rates may still be used to perform certain jobs but the average stiffness at lower sampling rates is higher than that of a higher sampling rate. Thus, H2M systems may require greater damping for stabilizing hard contacts. For teleoperation systems, kinesthetic information processing requires a thousand or more haptic data packets per second to be transferred between the master and the slave devices. Such a high packet rate will result in the use of large amounts of network resources in tandem with audio and video data transmission, leading to inefficient data communication. Therefore, in teleoperation systems, haptic data reduction or packet rate reduction becomes a necessity.

Some latest technical advancements that facilitate the realization of low-latency H2M and TI applications are software-defined networking (SDN), network function virtualization (NFV), and edge computing, to name a few. SDN is an important feature of 5G networks that decouples the control and data planes and provides centralized control of network elements. In a centralized control network, the management of traffic within a network becomes easier and mobility can be managed more efficiently [13] and with less latency while taking advantage of abstraction [14]. With NFV, virtualization and softwarization of network functions are possible that reduce the dependency on hardware, which in turn increases the reliability of the network and simplifies the sharing of resources among various network functions [15]. Edge computing solutions like cloudlets can play an important role in haptic communications where computations for stability control can be offloaded from the remote teleoperator [16]. By using the aforementioned NFV and cloudlets, "intelligence" can be efficiently distributed across network edges [17].

Note that the ultra-low latency communication between local master-slave pairs residing within the same wireless coverage area can be easily supported by advanced wireless technology such as 5G, WiFi, or Bluetooth. Nonetheless, data between remote master-slave pairs need to traverse through the optical front/back-haul segments [18]. Thus, it becomes challenging to meet the stringent latency requirements of H2M applications without being limited by the master-slave distance. This challenge can be overcome by preempting the haptic feedback from slave devices [19] and transmit this feedback from an intermediate artificial intelligence (AI)-enhanced H2M server. With this approach, the master receives the haptic feedback samples much quicker than the round-trip time of the master-slave pair and thus, remote H2M communications that meet stringent latency requirements can be deployed without being limited by the master-slave distance.

Recently, the authors of [20] proposed an edge sample forecast module that relies on historical data to forecast haptic feedback to the master. However, with this model, user experience can be significantly impacted by dynamic H2M applications where a certain diversity is present among various haptic feedback samples. Thus, in this paper, we propose an *Event-based HAptic feedback SAmple Forecast* (*EHASAF*) module that exploits a two-stage AI model consisting of an artificial neural network (ANN) unit followed by a reinforcement learning (RL) unit to forecast haptic feedback to the master. The ANN-based supervised learning unit decides when the master controller should start receiving haptic feedback samples and the RL unit ensures that the proper values of the haptic feedback samples are delivered. Thus, the master controller device receives proper haptic feedback samples within the expected quality of experience (QoE) time (D_Q). Moreover, the transmission of redundant haptic feedback samples is also reduced to a great extent. Our primary contributions in this paper are as follows:

- Firstly, we study various statistical characteristics of the control and haptic feedback data obtained from our virtual reality (VR) teleoperation experiments. We create histograms for various test scenarios from the

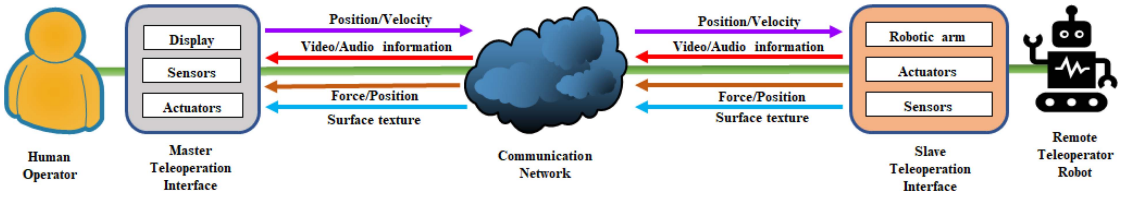

FIGURE 1. A schematic diagram of remote teleoperation showing communication between master and slave devices over a network.

packet arrival timestamps and successfully fit them with *generalized Pareto distribution* with optimal parameters.

- Secondly, we propose a two-stage AI-based haptic sample forecast unit, EHASAF. The first-stage uses ANN to implement a supervised learning algorithm on control signals from VR gloves to detect if forecasting of haptic feedback samples is necessary. We show that our designed ANN-based supervised learning algorithm can detect haptic feedback forecasting events from our experimental control signal data with $\sim 99\%$ accuracy.
- Thirdly, we propose a second-stage RL unit that uses a linear reward-inaction algorithm for run-time prediction of proper haptic feedback samples at every iteration. Through numerical evaluation, we perform a sensitivity analysis of the RL unit and investigate the impact of exploration and exploitation on the accuracy of the RL unit. Our results indicate $\sim 92\%$ accuracy for four different haptic materials with 90% mutual correlation in haptic feedback samples.
- Finally, we present the closed-loop latency for data transmission between master and slave devices over an optical fiber backhaul network against the overall network traffic intensity. In this context, we show that the deployment of remote H2M teleoperation is infeasible for a 40 km master-slave closed-loop network with more than 65% overall traffic intensity. However, such deployment is possible by using our proposed EHASAF module with an intermediate H2M server.

The rest of this paper is organized as follows. In Section II, we review some recent works done in this area. In Section III, we briefly discuss our considered network architecture to facilitate remote H2M applications. In Section IV, the details of our experimental setup, the ANN-based binary classifier unit and the RL unit are presented. In Section V, the performance of the proposed EHASAF module is evaluated. Finally, in Section VI, our primary observations and achievements by using the proposed EHASAF module are summarized.

II. RELATED WORKS

In this section, we review recent research related to bilateral teleoperation over TI network infrastructures. We keep the focus of our discussions on ultra-reliable low-latency communications (uRLLC) and H2M applications. A comprehensive survey on uRLLC related research and standards like IEEE time sensitive network (TSN) and IETF deterministic networks (DetNet) is given in [21]. The primary objective of both TSN and DetNet is to define a common network architecture that realizes uRLLC while meeting some guaranteed bounds on latency, jitter, and packet loss. In [22], the authors provided an overview of TI services and haptic communications and thoroughly discussed the 5G functionalities that can achieve guaranteed low-latency transmission over wireless networks. The authors of [23] proposed a single-cell sparse multiple-access wireless network resource assignment system that would optimize the data transmission rates for haptic users subject to transmission power and latency constraints. The authors of [24] proposed a time-division packet drop mechanism for duplexing cellular systems that satisfies the quality-of-service (QoS) requirements of the finite transmitting power and optimizes the queue state information and the transmission policy by depending on channel state information. For achieving low per-packet in-order delivery delays for 5G and TI applications, the authors of [25] proposed a low-complexity Stochastic Earliest Delivery Path First (S-EDPF) protocol while considering uncertainty and time-variation in path delays. Moreover, the authors of [26] analyzed TI and discussed the system design of uRLLC in new radio (NR) and long-term evolution (LTE) technologies from a physical layer and medium-access control perspective.

The next important aspect and challenge is to enhance the human operators' QoE, following the design of uRLLC networking infrastructures that lays the foundation for the TI. Only when the human operator obtains sufficient multimodal sensory feedback, especially the sense of touch, a real immersion in the remote environment possible. In this context, the authors of [27] applied skin deformation feedback on multiple fingerpads that provide multi-degree-of-freedom interaction force direction and magnitude information to human operators and showed improvement in performance and QoE. In [28], the authors explored the robotic embodiment by employing augmented reality feedback to the human operators that allows them to execute tasks with better accuracy, dexterity, and visualization. The authors of [31] introduced Tactile Robots (TR) as the next evolutionary step in robotic systems and described the enabling technologies for the embodiment of the TI via smart wearables. In [30], the authors conducted a trace-driven study for proposing a multi-sample-ahead-of-time sample forecasting scheme that compensates for the delay in haptic feedback samples over FiWi networks. Some researchers aimed at multi-robot task allocation for the TI, e.g., the authors of [29] presented a task allocation strategy which provides a suitable host robot selection and computation offloading to collaborative nodes. Furthermore, the authors of [32] used mixed-integer programming techniques for solving single

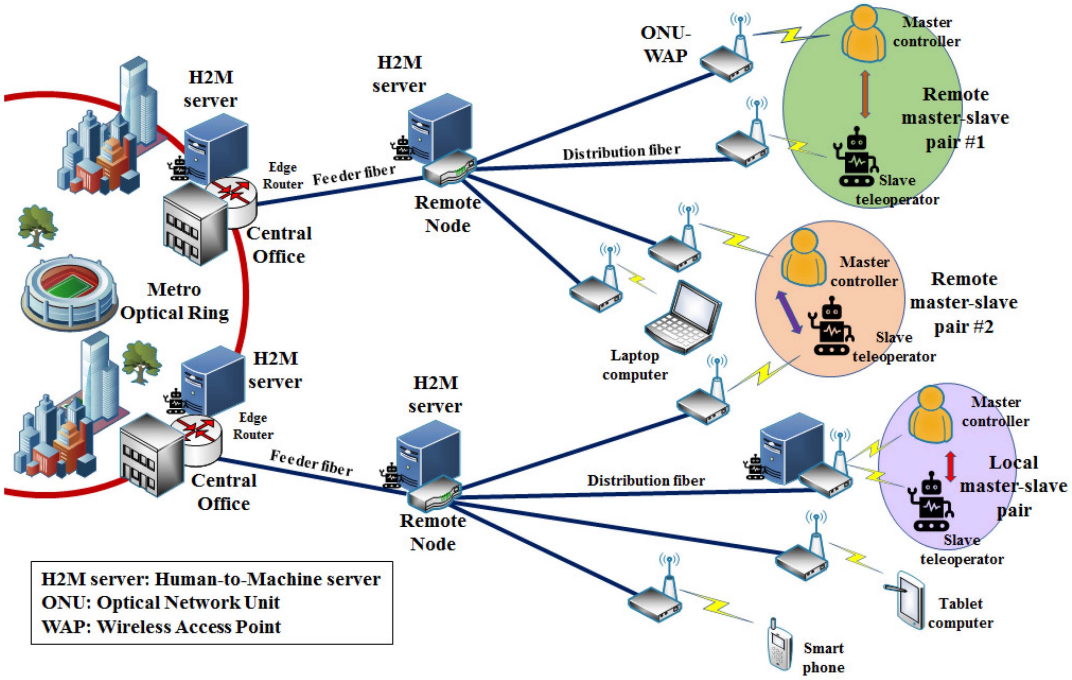

FIGURE 2. Local and remote teleoperation master-slave pairs using H2M servers over TDM or WDM-PON based FiWi networks.

TABLE 1. Comparison with existing tactile Internet works.

Papers	Network applications	Proposed idea	Haptic feedback preemption
[27]	Real-time telesurgery	Applied a coupled tangential and normal skin deformation feedback to human teleoperators for a precision grip using multiple fingerpads	Did not attempt to address network issues related to remote teleoperation use cases; no consideration of haptic feedback preemption
[28]	AR-based teleoperation	Employed AR feedback to human operators that allows them to execute teleoperation tasks with better accuracy, dexterity, and visualization	Did not attempt to address network issues related to remote teleoperation use cases; no consideration of haptic feedback preemption
[29]	Real-time teleoperation	Presented a task allocation strategy which provides a suitable host robot selection and computation offloading to collaborative nodes	Attempted to minimize end-to-end latency by choosing a suitable collaborative computational node; no consideration of haptic feedback preemption
[30]	Real-time teleoperation	Proposed a multi-sample-ahead-of-time sample forecasting scheme that compensates for the delay in haptic feedback samples over FiWi networks	Attempted to minimize end-to-end latency through efficient task scheduling and assignment algorithms; no consideration of haptic feedback preemption
[20]	Real-time teleoperation	Proposed an edge sample forecast module that relies on historical data to forecast haptic feedback to the human operator interface	Used an ANN to forecast haptic feedback samples; no consideration of forecasting of haptic feedback samples when different types of materials are present
Our paper	VR-based teleoperation	Proposed a two-stage AI unit consisting of a cascaded ANN and RL unit to forecast haptic feedback to the master for multiple materials	Used an ANN to start/stop forecasting of haptic feedback and an RL unit to dynamically explore haptic feedback samples of different materials

robot task planning problems. In Table 1, we highlight the primary contributions of our current paper over some of the aforementioned works.

III. HUMAN-TO-MACHINE NETWORK ARCHITECTURE

Fig. 2 illustrates an example of network architecture where different combinations of *local and remote H2M master-slave pairs* are connected over FiWi access networks. The wireless access points (WAP) are integrated with optical network units (ONUs) of a time division multiplexed (TDM) or wavelength division multiplexed (WDM) passive optical network (PON) as fiber backhaul network. The ONUs in a typical PON is situated at a distance of 10-20 km from the central office (CO) and the distance is nearly 100 km for long-reach PON. For local H2M teleoperation (shown by the purple circle), the intermediate distance between master and slave devices is very short, usually, a few meters and hence, wireless technologies like 5G new radio, WiFi, or Bluetooth can support them. However, when we consider remote H2M teleoperation scenarios like *intra-PON master-slave devices* (shown by the green circle) and *inter-PON master-slave devices* (shown by the pink circle), then relying on optical front/back-haul segments becomes essential [33].

It is important to note that the end-to-end propagation latency still presents a bottleneck for remote H2M teleoperation scenarios as light cannot travel faster than 2×10^8 m/s within an optical fiber. If each of the master and slave devices is connected to an ONU of a 100 km long-reach PON,

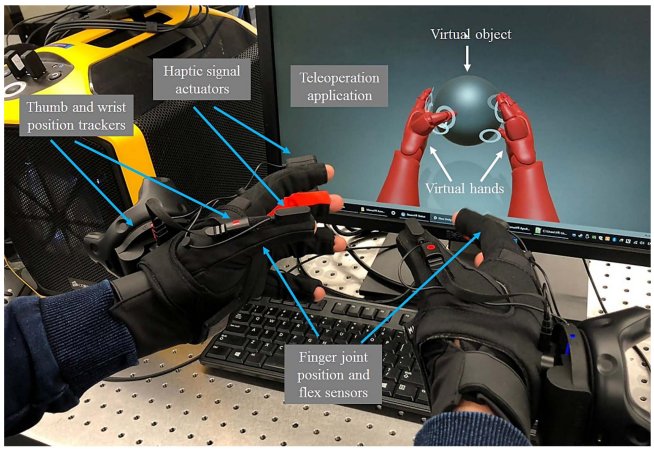

(a) Various components of VR based H2M teleoperation experimental setup.

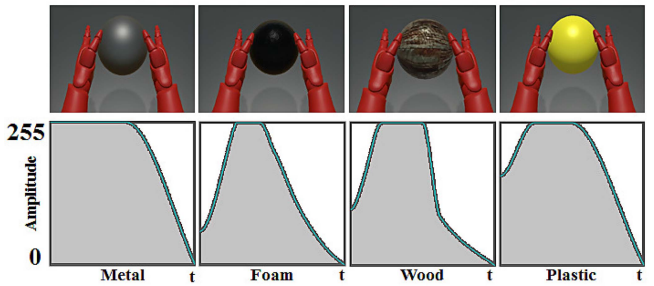

(b) Haptic feedback samples for different types of material [34].

FIGURE 3. Different components of VR H2M experimental setup and haptic feedback samples corresponding to different types of material.

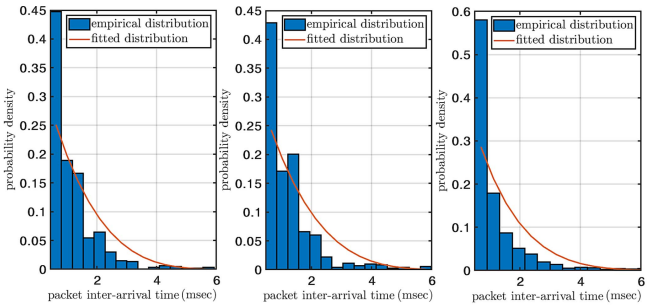

(a) Control signals for grab a ball, a cube, and a circular cube, respectively.

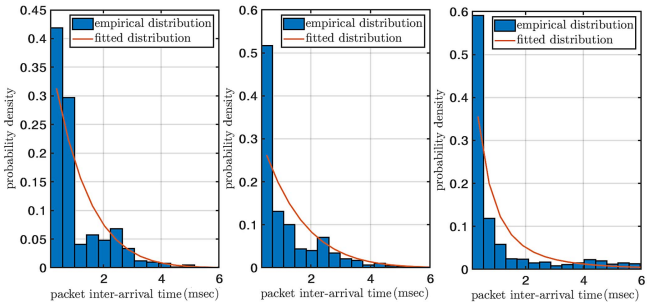

(b) Haptic feedback for grab a ball, a cube, and a circular cube, respectively.

FIGURE 4. Distribution fitting corresponding to empirical histograms of timestamps of control signals and haptic feedback from different tests.

then only the end-to-end propagation latency becomes 1 ms. Nonetheless, such remote H2M teleoperations can be made feasible with various AI-enhanced edge-computing servers to predict bandwidth demands or forecast haptic samples, indicated as "H2M server" in Fig. 2. These H2M servers can be installed at the network edge to support a group of ONUs, or at the remote node or CO, depending on given cost, bandwidth, and latency constraints.

IV. SYSTEM MODEL

In this section, we briefly describe our VR based H2M experimental setup and the statistical characteristics of control and haptic feedback signals. Then we discuss the EHASAF module consisting of a supervised learning algorithm implemented by an ANN unit to predict if haptic feedback samples required to be forecasted, followed by an RL algorithm to forecast proper haptic feedback samples to the master device.

A. EXPERIMENTAL SETUP AND NETWORK STATISTICS

In any H2M experimental setup, the hardware design parameters like sampling frequency, the number and type of sensors and actuators determine the volume of input and output data [35]. The slave haptic subsystem can either be a physical device interacting with a remote physical environment or a virtual pointer like a virtual hand, operating in a virtual environment. Simulated virtual worlds are hassle-free to reproduce and can allow connectivity with multiple users to communicate with each other in a virtual space over a local network or the Internet in some situations. To study the characteristics of the control signals from a master device and the corresponding haptic signals from a slave device, we created a VR based H2M experimental setup as shown in Fig. 3(a).

The master device consists of a pair of VR gloves and each glove has two orientation sensors on the thumb and wrist with 9 degrees-of-freedom, and five flexible sensors on five fingers for tracking movements and applied forces [36]. The sensor sampling rate is 200 Hz and the control signals are transmitted over a wireless interface to the computer where a VR application for touching a virtual ball (the slave device) is run. The wireless interface is a customized Bluetooth interface that can support a maximum master-slave distance of 30 meters [36]. Quaternion and Euler's angles are used to record the thumb, wrist, and finger joints' orientation data [37]. Moreover, two flex sensors per finger record the normalized tension on each finger. Hence, each instance of control signal from either hand contains a total of $(4 \times 2) + (5 \times 5 \times 3) + (5 \times 2) = 93$ elements. When any finger touches the virtual ball and depending on the type of material of the ball, e.g., metal, foam, wood, or plastic, the VR application sends different haptic feedback samples to the haptic actuators of the corresponding finger. The haptic feedback samples, with amplitude values that lie within 0 to 255, as shown in Fig. 3(b), are transmitted to the master device within 100 ms. The signal latency of the haptic feedback is 10 ms and the maximum force felt is 0.9 gram-force [36].

To characterize the traffic pattern of control signals and haptic feedback of VR based H2M teleoperation, we perform

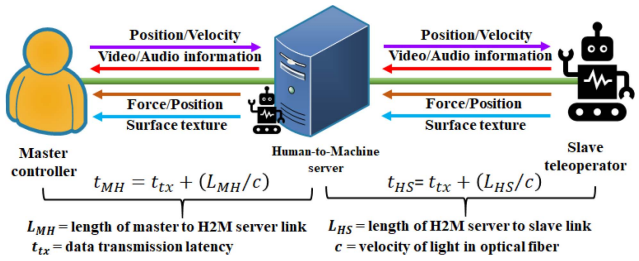

FIGURE 5. Logical links between master, H2M server, and slave devices.

three different test scenarios in our experimental setup, e.g., grabbing a virtual ball, grabbing a virtual cube, and grabbing a virtual circular cube (cube with circular facets). The histograms obtained from the timestamps of control signals for all three test scenarios are shown in Fig. 4(a). Similarly, the histograms obtained from the timestamps of haptic feedback for all three test scenarios are shown in Fig. 4(b). Note that we scaled these histograms from a mean of 10 ms to 1 ms for compatibility with standard H2M teleoperation QoE requirements. We observe that all these distributions well fit a *generalized Pareto distribution* [38]. Recall that the probability density function $f_X(\cdot)$ of a generalized Pareto distribution X with shape parameter $k \neq 0$, scale parameter σ, and threshold parameter θ is given by:

$$f_X(x|k,\sigma,\theta) = \left(\frac{1}{\sigma}\right)\left(1 + k\frac{(x-\theta)}{\sigma}\right)^{-1-\frac{1}{k}}, \tag{1}$$

for $\theta < x$, if $k > 0$, or for $\theta < x < (\theta - \frac{\sigma}{k})$ if $k < 0$. For $k = 0$, the density becomes an *exponential distribution* as follows:

$$f_X(x|0,\sigma,\theta) = \left(\frac{1}{\sigma}\right)\exp\left(-\frac{(x-\theta)}{\sigma}\right), \tag{2}$$

for $\theta < x$. The optimal distribution parameter values in terms of goodness-of-fit, empirical and fitted means and variances are summarized in Table 2. We also ensure through *Chi-square goodness-of-fit (GoF)* test that the distribution fittings are accurate with a 5% significance level.

B. AI-BASED HAPTIC FEEDBACK SAMPLE FORECAST MODULE

We consider the case in which H2M server is situated between the master and slave devices and hence, the network is divided into two logical segments, i.e., master-H2M server (MH) and H2M server-slave (HS), as shown in Fig. 5. We denote the latency between master and H2M server as t_{MH} and the latency between the H2M server and slave as t_{HS}. Hence, the total end-to-end latency between control signal generation at the master device and reception of the corresponding haptic signal is $D_{MS} = 2\times(t_{MH}+t_{HS})$. However, if $D_{MS} > D_Q$, then the user experience degrades. To overcome this issue, we install the proposed EHASAF module in the H2M server that acts as a proxy of the slave device.

(a) EHASAF - ANN Unit: The first stage of the EHASAF module is an ANN unit corresponding to each of the thumb, index, middle, ring, and baby fingers of both hands (as shown in Fig. 6) and detects each finger's actions, i.e., whether it is going to touch the virtual object or not. A typical ANN can be viewed as *a universal approximator, which can approximate any linear/non-linear function to any arbitrary degree of accuracy* [39]. Therefore, an ANN can be used for function approximation, regression analysis, and data classification. Usually, there are multiple hidden layers in an ANN, consisting of a network of artificial neurons to represent a linear combination of certain parameterized non-linear functions. During the training phase, the weights of the interconnections among the neurons are determined based on the trained data. Once the network is fully trained, the ANN can be used for producing a suitable output based on any input data. From our VR based H2M experiments, the wrist and thumb coordinates and the rotation and tension of each finger are considered as inputs to the ANN. The ANN corresponding to each finger uses supervised learning algorithms to act as a *binary classifier*. These ANNs try to minimize the mean-squared error (MSE) in the classification [40] and the outputs of each ANN are "touch" or "no-touch." Thus, the training data for each ANN corresponding to each finger can be considered a vector of $(5\times 3)+2 = 17$ elements and we denote it by $\boldsymbol{x}$. The output of the classifier is denoted by a variable $y \in \{\text{touch, no-touch}\}$ and $\boldsymbol{w}$ denotes the weight parameter vector. Therefore, for a set of input vectors $\{\boldsymbol{x}_n\}$, where $n = 1,\ldots,N$ and a corresponding set of labels $\{t_n\}$, we minimize the MSE function as follows:

$$\mathbb{E}(w) = \frac{1}{2}\sum_{n=1}^{N}\{y(\boldsymbol{x}_n,\boldsymbol{w}) - t_n\}^2. \tag{3}$$

As our multi-layer ANN uses forward-propagation and backward-propagation methods to implement this binary classifier, the time-complexity is given by $\mathcal{O}(n_0n_1 + n_1n_2 + \cdots + n_in_{i+1} + \ldots)$, where n_i is the number of neurons in the i^{th} layer [4]. This complexity can be further improved by some specialized training algorithms like the *Levenberg-Marquardt algorithm*, which does not compute the exact Hessian matrix but, computes the gradient vector and the Jacobian matrix [41]. With a cost function like MSE, that has the form of a sum of squares, the Hessian matrix can be approximated as $H = J^TJ$ and the gradient can be computed as $g = J^Te$, where J is the Jacobian matrix that contains first derivatives of the network errors with respect to the weights and biases, and e is a vector of network errors. With this approximation of the Hessian matrix, the Levenberg-Marquardt algorithm reduces to the following Newton-like update rule:

$$x^{(k+1)} = x^{(k)} - \left[J^TJ + \mu I\right]^{-1}J^Te. \tag{4}$$

When the scalar μ is equal to zero, then (4) is the same as Newton's method but, when $\mu > 0$, then (4) reduces to a gradient descent algorithm with a small step size. As Newton's method is very fast and highly accurate near an error minimum, we aim to shift towards Newton's method

TABLE 2. Generalized Pareto distribution fitting corresponding to control signals and haptic feedback timestamp histograms.

	Grab a ball		Grab a cube		Grab a circular cube	
	Control signal	Haptic feedback	Control signal	Haptic feedback	Control signal	Haptic feedback
k	-0.2017 [-0.2390, -0.1644]	-0.1145 [-0.1426, -0.08633]	-0.1999 [-0.2395, -0.1603]	-0.1100 [-0.1312, -0.08883]	-0.1422 [-0.1768, -0.1077]	+0.4618 [0.3904, 0.5332]
σ	+0.001391 [0.001280, 0.001512]	+0.001150 [0.001099, 0.001204]	+0.001456 [0.001342, 0.001579]	+0.001306 [0.001251, 0.001364]	+0.001332 [0.001242, 0.001428]	+0.00073 [0.00067, 0.00079]
θ	0	0	0	0	0	0
Histogram mean	0.001183615615615	0.001034569892473	0.001235497267759	0.001182086891942	0.001178701740812	0.001271528073916
Distribution mean	0.001158180137842	0.001032717179577	0.001213301782568	0.001176983051996	0.001166483139090	0.001356732115846
Histogram variance	$5.9957417984\times10^{-07}$	$5.9957417984\times10^{-07}$	7.00931861×10^{-07}	$9.9095864475\times10^{-07}$	$7.6875969728\times10^{-07}$	$3.2054223432\times10^{-06}$
Distribution variance	$9.5572064513\times10^{-07}$	$8.6776193696\times10^{-07}$	1.05159692×10^{-06}	$1.1354124842\times10^{-06}$	$1.0592440674\times10^{-06}$	$2.4129239902\times10^{-05}$
Chi-square GoF (5 %)	✓	✓	✓	✓	✓	✓

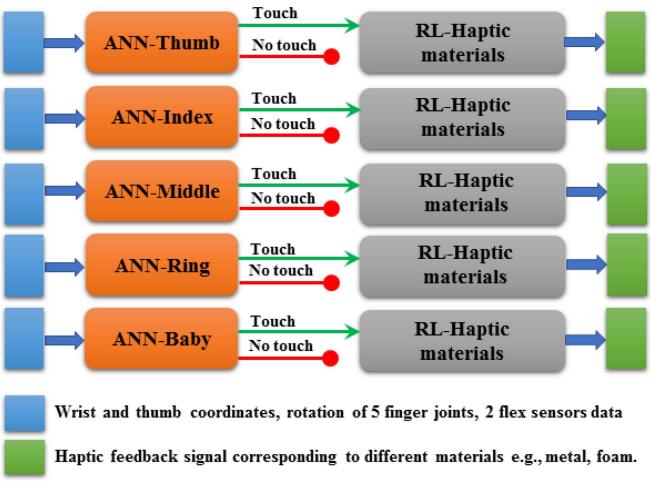

FIGURE 6. AI-based EHASAF module with cascaded ANN and RL units.

as soon as possible. To achieve this, we decrease μ after each successful step and increase after a step if there is an increase in the MSE cost function. In this way, the MSE cost function is always reduced at each iteration of the algorithm. Note that, this complexity is applicable only for the training or calibration phase and does not affect the run-time complexity of the system. If it is a no-touch event, then no immediate haptic feedback is required to be transmitted to the master. However, when any finger touches the object, the EHASAF module starts to generate haptic samples every $(D_Q - t_{MH})$ interval. Therefore, the master device receives a haptic feedback sample after every D_Q interval, satisfying both user experience and network latency constraints.

(b) EHASAF - RL Unit: If there are different types of material involved, it is important to correctly forecast the corresponding haptic feedback samples. Hence, we implement an RL unit that uses a customized *linear reward-inaction algorithm* for this purpose [42]. When a finger touch is detected by the ANN at i^{th} time-slot, the RL units randomly chooses a material $(m_k^{(i)})$, where $k \in \{1, \ldots, K\}$, and forecasts the first haptic feedback sample. To forecast the haptic feedback sample correctly, initially, the RL unit uses its prior knowledge of haptic feedback profiles of all the materials. After every $(t_{MH}+2\times t_{HS})$ interval, the H2M server receives the actual haptic feedback sample from the slave device and computes the reward $(r^{(i)})$, which is then normalized error in haptic sample forecasting. With this reward value, the RL unit updates its probability distribution for choosing a haptic material in the $(i+1)^{\text{th}}$ timeslot. When $(2 \times D_Q - t_{MH}) \geq (t_{MH} + 2 \times t_{HS})$, then the H2M server receives the haptic feedback sample before generating the next haptic sample and the RL unit works at its best; otherwise, the RL unit takes more time to detect the actual material and the user experience consequently degrades. As we are forecasting haptic feedback samples, hence we are gaining an additional time buffer of D_Q interval. A summary of the working principle of the RL unit, if a touch event is detected by ANN at the i^{th} time-slot, is given in the following:

(i) The RL unit randomly chooses a material $(m_k^{(i)})$ from all possible K materials.

(ii) We denote the haptic feedback sample chosen by the RN unit at i^{th} time-slot by $h_{HM}^{(i)}$ and the actual haptic sample generated at the slave device by $h_{SM}^{(i)}$. Thus, we define the value of the reward received at the H2M server as $r^{(i)} = |h_{SM}^{(i)} - h_{HM}^{(i)}|/255$, such that $0 \leq r^{(i)} \leq 1$.

(iii) The probability distribution of the RL unit for choosing a material in $(i+1)^{\text{th}}$ timeslot is updated according to the following update rule:

$$\boldsymbol{p}_m^{(i+1)} = \boldsymbol{p}_m^{(i)} + \alpha r^{(i)} \left(\boldsymbol{e}_k^{(i)} - \boldsymbol{p}_m^{(i)} \right), \tag{5}$$

where $0 \leq \alpha \leq 1$ is the *learning rate parameter* and $\boldsymbol{e}_k^{(i)}$ is an *indicator vector* with unity at the k^{th} index.

Note that (5) is a linear reward-inaction automaton and this algorithm shows very strong convergence properties in practice. As it is an RL-based algorithm, it relies on commonly used *exploration* and *exploitation* mechanisms [42]. A smaller value of α indicates more weight on exploration whereas a larger value of α indicates more weight on exploitation. As an example case, we consider the four haptic feedback profiles shown in Fig. 3(b) that has nearly 75% degree of similarity based on the mutual correlation

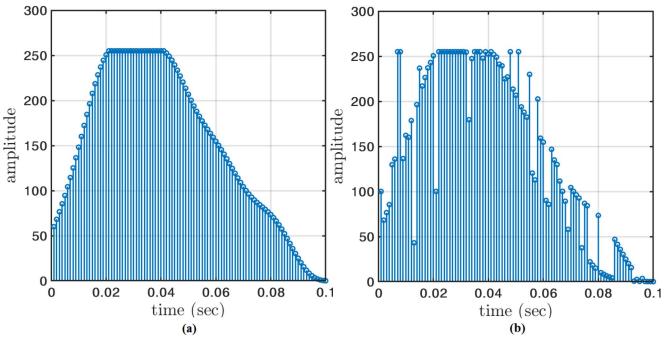

FIGURE 7. (a) Actual haptic feedback samples and (b) RL unit forecasted haptic feedback samples.

among themselves. Fig. 7a shows the actual haptic feedback samples generated by the slave devices. If we choose $\alpha = 1$, i.e., aggressive exploitation and less exploration, then an instance of the RL unit forecasted haptic feedback samples are shown in Fig. 7b. In this case, the forecasted samples are 92.59% accurate to the actual haptic feedback samples.

V. PERFORMANCE EVALUATION

In this section, we evaluate the performance of our proposed EHASAF module. From our experimental setup, we collected several instances of both control signal and haptic feedback data of all the experiments, i.e., grabbing a virtual ball, a virtual cube, and a circular cube of different materials with both hands. We implemented an ANN in MATLAB that contains 2 hidden layers with 10 and 5 nodes, respectively, and used the *Levenberg–Marquardt training method* for training because of its faster convergence rate as compared to conventional gradient descent algorithms for moderate-sized feedforward neural networks [41]. Fig. 8 shows the accuracy of the binary classification performed by the ANN with the control data from 800 instances of "grabbing a virtual ball" test scenario. The mean square error decreases gradually with the number of epochs. We used 70% of the data for training, 15% data for validation, and 15% for testing to achieve a prediction accuracy of $\sim 99\%$. A similar degree of accuracy was also observed in the other test scenarios.

When the ANN detects a finger touching the virtual ball, the EHASAF module starts to generate and forecast haptic feedback samples. With only one material involved in the testing, the feedback is 100% correct, but if there are multiple materials to choose, then the accuracy of the forecasted haptic feedback samples decreases. In Fig. 9, we consider that the learning rate parameter (α) varies from 0.1 to 1.0 and four sets of data that have an average degree of similarity in terms of average mutual correlation coefficient 0.25, 0.50, 0.75, and 0.90, respectively. The total duration of each haptic feedback burst is 100 ms and consequent samples are forecast after every 1 ms interval. We observe that the average haptic feedback sample forecasting accuracy increases as the degree of similarity increases. It is also interesting to

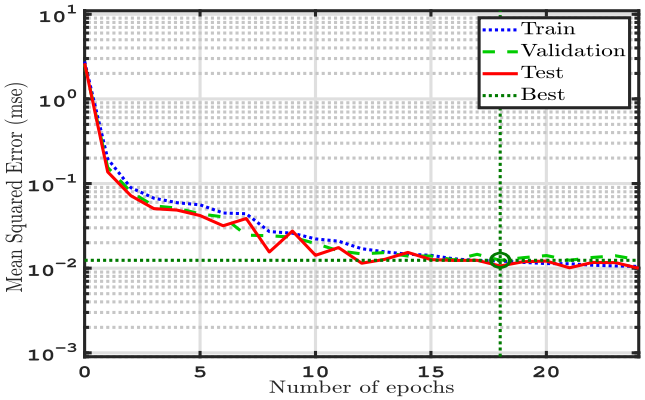

FIGURE 8. Accuracy of binary classification implemented by ANN.

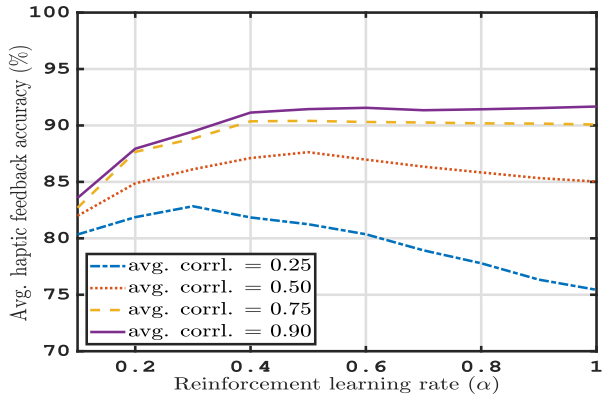

FIGURE 9. RL forecasted haptic feedback accuracy vs. parameter α.

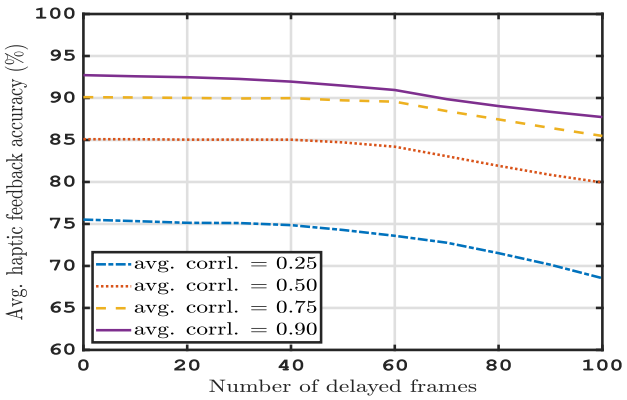

FIGURE 10. RL forecasted haptic feedback accuracy vs. frame delay.

observe that, when the degree of similarity is lower, more exploration provides relatively better accuracy, whereas when the degree of similarity is higher, then a better accuracy is achieved through more exploitation.

In order to extract the best performance from the RL unit, at every iteration, each actual haptic feedback sample from the slave device must reach the H2M server before the generation of the next haptic feedback sample. If we can ensure that $(2 \times D_Q - t_{HM}) \geq (t_{MH} + 2 \times t_{HS})$, then the H2M server receives the haptic feedback samples before

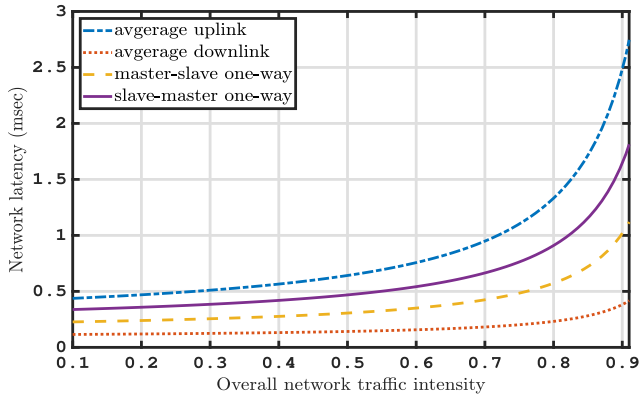

FIGURE 11. End-to-end network latency over fiber backhaul vs. overall traffic intensity of a 20 km 1G-EPON with 16 ONUs.

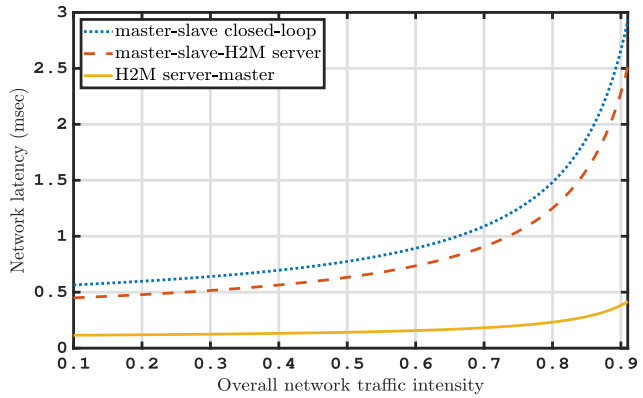

FIGURE 12. Comparison of closed-loop master-slave network latency vs. master-slave-H2M server latencies over fiber backhaul.

generating the next haptic sample and the RL unit works at its best; otherwise, the RL unit takes more time to detect the actual material and the user experience consequently degrades. Thus, in Fig. 10 we observe the impact of delay in receiving haptic feedback samples from the slave device to H2M server, where each number of delayed frames implies 1 ms delay. Nonetheless, we observe that the accuracy of the RL unit does not degrade very drastically, rather gradually. This implies that the EHASAF module is quite robust in terms of handling delay in packet arrivals. Even when the network is overloaded and the master-slave packet delay is significant, the EHASAF module still ensures that the master receives reasonably accurate haptic feedback samples within every D_Q interval.

To investigate the end-to-end latency between master and slave devices over a TDM-PON based fiber backhaul, we consider a 20 km 1G-EPON with 16 ONUs. We consider that a master device is directly connected to an ONU and a slave device is connected to another ONU. The remaining 14 ONUs are transmitting Poisson distributed background traffic. We use optimal distribution fitting parameter values from Section IV to characterize the control signal and haptic feedback traffics. The master device transmits only control signals with a packet size of 100 B and a bandwidth of 16 Mbps is required for both the gloves. On the other hand, the slave device transmits 360° video and audio data along with haptic feedback [43]. The video data has a packet size of 1.5 kB and requires a bandwidth of 30 Mbps (average) to 60 Mbps (maximum). The audio data has a packet size of 100 B and requires a bandwidth of 512 Kbps. The haptic feedback data has a packet size of 80 B and requires a bandwidth of 1.28 Mbps. With this configuration, the intermediate distance between the master and slave devices is $20 + 20 = 40$ km and the end-to-end propagation latency is 0.2 ms. We consider that the H2M server is situated at the CO and hence, its distance from both the master and slave is 20 km with a propagation latency of 0.1 ms. For computing the average uplink and downlink network latency of the fiber backhaul, we refer to the analytical expressions derived in [44] and whereby the authors previously verified the accuracy of these expressions through network simulations.

In Fig. 11, we show the average uplink and downlink latencies of all the ONUs. We also show the one-way latencies of the master-slave and slave-master paths in this figure. The results indicate that when the overall network traffic intensity, i.e., background plus H2M traffic intensity is more than 80%, then the slave to master latency exceeds 1 ms. Furthermore, in Fig. 12 we compare the closed-loop master-slave latency with the latency of master to slave and slave to H2M server. We observe that the closed-loop master-slave latency exceeds 1 ms when the overall network traffic intensity is higher than 65%. In this case, remote H2M teleoperation can not be implemented because the haptic feedback samples from the slave device will reach later than 1 ms to the master device. However, the latency between the H2M server and the master device remains below 0.5 ms even with 90% overall network traffic intensity. Therefore, our results indicate that we can still implement remote H2M teleoperation by using our proposed EHASAF module in the H2M server at the CO.

VI. CONCLUSION

The primary objective of this paper is to facilitate remote H2M applications with AI-enhanced servers over FiWi access networks. We believe that our contributions are fundamental that will encourage more future research on edge-intelligence for immersive TI communications [45]. In this paper, we have fitted generalized Pareto distribution with optimal parameter values to the histograms obtained from the timestamps of control signals and haptic feedback from three different VR based H2M teleoperation test scenarios. To deploy remote H2M teleoperation, we have proposed the idea of installing AI-enhanced H2M server between master and slave devices that supports the preemption of haptic feedback from control signals. Moreover, we have proposed a two-stage AI-based EHASAF module to forecast haptic feedback samples from the H2M server to the master device. The first stage of the EHASAF module is a supervised learning unit that implements a binary classifier by using an ANN to detect if haptic sample forecasting is necessary with $\sim 99\%$

accuracy. The second stage of the EHASAF module is a reinforcement learning unit that ensures $\sim 90\%$ accuracy in the forecasted haptic feedback samples with four different types of material and average mutual correlation coefficient of 0.9. We have also ensured that the EHASAF module is robust in terms of delayed packet arrivals. Finally, by using analytical expressions for fiber backhaul latency, we show the feasibility of deploying remote H2M teleoperation over a 20 km 1G-EPON with 16 ONUs by using our proposed EHASAF module in an intermediate H2M server, even under heavy traffic intensity.

ACKNOWLEDGMENT

The authors thank Prof. Larrabeiti for hosting S. Mondal and M. Maier in Charles III University of Madrid.

REFERENCES

[1] G. P. Fettweis, "The Tactile Internet: Applications and challenges," *IEEE Veh. Technol. Mag.*, vol. 9, no. 1, pp. 64–70, Mar. 2014.
[2] M. Dohler *et al.*, "Internet of skills, where robotics meets AI, 5G and the Tactile Internet," in *Proc. Eur. Conf. Netw. Commun. (EuCNC)*, 2017, pp. 1–5.
[3] O. Holland *et al.*, "The IEEE 1918.1 'Tactile Internet' standards working group and its standards," *Proc. IEEE*, vol. 107, no. 2, pp. 256–279, Feb. 2019.
[4] L. Ruan, M. P. I. Dias, and E. Wong, "Enhancing latency performance through intelligent bandwidth allocation decisions: A survey and comparative study of machine learning techniques," *J. Opt. Commun. Netw.*, vol. 12, no. 4, pp. B20–B32, Apr. 2020.
[5] M. Maier, M. Chowdhury, B. P. Rimal, and D. P. Van, "The Tactile Internet: Vision, recent progress, and open challenges," *IEEE Commun. Mag.*, vol. 54, no. 5, pp. 138–145, May 2016.
[6] S. J. Lederman and R. L. Klatzky, "Haptic perception: A tutorial," *Attention Perception Psychophys.*, vol. 71, no. 7, pp. 1439–1459, Oct. 2009.
[7] K. Antonakoglou, X. Xu, E. Steinbach, T. Mahmoodi, and M. Dohler, "Toward haptic communications over the 5G Tactile Internet," *IEEE Commun. Surveys Tuts.*, vol. 20, no. 4, pp. 3034–3059, 4th Quart., 2018.
[8] J.-Y. Lee and S. Payandeh, *Haptic Teleoperation Systems: Signal Processing Perspective*. Cham, Switzerland: Springer, 2015.
[9] D. A. Lawrence, "Stability and transparency in bilateral teleoperation," *IEEE Trans. Robot. Autom.*, vol. 9, no. 5, pp. 624–637, Oct. 1993.
[10] J. E. Colgate and G. Schenkel, "Passivity of a class of sampled-data systems: Application to haptic interfaces," in *Proc. Amer. Control Conf. (ACC)*, vol. 3, Jun. 1994, pp. 3236–3240.
[11] J. J. Abbott and A. M. Okamura, "Effects of position quantization and sampling rate on virtual-wall passivity," *IEEE Trans. Robot.*, vol. 21, no. 5, pp. 952–964, Oct. 2005.
[12] N. Diolaiti, G. Niemeyer, F. Barbagli, and J. K. Salisbury, "Stability of haptic rendering: Discretization, quantization, time delay, and coulomb effects," *IEEE Trans. Robot.*, vol. 22, no. 2, pp. 256–268, Apr. 2006.
[13] T. Mahmoodi and S. Seetharaman, *On Using a SDN-Based Control Plane in 5G Mobile Networks*, Wireless World Res. Forum, Frankfurt, Germany, 2014.
[14] A. C. Morales, A. Aijaz, and T. Mahmoodi, "Taming mobility management functions in 5G: Handover functionality as a service (FaaS)," in *Proc. IEEE Globecom Workshops (GC Wkshps)*, Dec. 2015, pp. 1–4.
[15] I. Giannoulakis, E. Kafetzakis, G. Xylouris, G. Gardikis, and A. Kourtis, "On the applications of efficient NFV management towards 5G networking," in *Proc. 1st Int. Conf. 5G Ubiquitous Connectivity*, Nov. 2014, pp. 1–5.
[16] A. A. Dyumin, L. A. Puzikov, M. M. Rovnyagin, G. A. Urvanov, and I. V. Chugunkov, "Cloud computing architectures for mobile robotics," in *Proc. IEEE NW Russia Young Res. Elect. Electron. Eng. Conf. (EIConRusNW)*, Feb. 2015, pp. 65–70.
[17] E. Wong, M. P. I. Dias, and L. Ruan, "Predictive resource allocation for Tactile Internet capable passive optical LANs," *J. Lightw. Technology*, vol. 35, no. 13, pp. 2629–2641, Jul. 2017.
[18] L. Ruan, M. P. I. Dias, M. Maier, and E. Wong, "Understanding the traffic causality for low-latency human-to-machine applications," *IEEE Netw. Lett.*, vol. 1, no. 3, pp. 128–131, Sep. 2019.
[19] M. A. Lema, T. Mahmoodi, and M. Dohler, "On the performance evaluation of enabling architectures for uplink and downlink decoupled networks," in *Proc. IEEE Globecom Workshops (GC Wkshps)*, Dec. 2016, pp. 1–6.
[20] M. Maier and A. Ebrahimzadeh, "Towards immersive Tactile Internet experiences: Low-latency FiWi enhanced mobile networks with edge intelligence [invited]," *IEEE/OSA J. Opt. Commun. Netw.*, vol. 11, no. 4, pp. B10–B25, Apr. 2019.
[21] A. Nasrallah *et al.*, "Ultra-low latency (ULL) networks: The IEEE TSN and IETF DetNet standards and related 5G ULL research," *IEEE Commun. Surveys Tuts.*, vol. 21, no. 1, pp. 88–145, 1st Quart., 2019.
[22] J. Sachs *et al.*, "Adaptive 5G low-latency communication for Tactile Internet services," *Proc. IEEE*, vol. 107, no. 2, pp. 325–349, Feb. 2019.
[23] N. Gholipoor, H. Saeedi, and N. Mokari, "Cross-layer resource allocation for mixed tactile Internet and traditional data in SCMA based wireless networks," in *Proc. IEEE Wireless Commun. Netw. Conf. Workshops (WCNCW)*, 2018, pp. 356–361.
[24] C. She, C. Yang, and T. Q. S. Quek, "Cross-layer transmission design for Tactile Internet," in *Proc. IEEE Global Commun. Conf. (GLOBECOM)*, 2016, pp. 1–6.
[25] A. Garcia-Saavedra, M. Karzand, and D. J. Leith, "Low delay random linear coding and scheduling over multiple interfaces," *IEEE Trans. Mobile Comput.*, vol. 16, no. 11, pp. 3100–3114, Nov. 2017.
[26] C. Li *et al.*, "5G-based systems design for Tactile Internet," *Proc. IEEE*, vol. 107, no. 2, pp. 307–324, Feb. 2019.
[27] Z. F. Quek, W. R. Provancher, and A. M. Okamura, "Evaluation of skin deformation tactile feedback for teleoperated surgical tasks," *IEEE Trans. Haptics*, vol. 12, no. 2, pp. 102–113, Apr.–Jun. 2019.
[28] F. Brizzi, L. Peppoloni, A. Graziano, E. D. Stefano, C. A. Avizzano, and E. Ruffaldi, "Effects of augmented reality on the performance of teleoperated industrial assembly tasks in a robotic embodiment," *IEEE Trans. Human–Mach. Syst.*, vol. 48, no. 2, pp. 197–206, Apr. 2018.
[29] M. Chowdhury and M. Maier, "Collaborative computing for advanced Tactile Internet human-to-robot (H2R) communications in integrated FiWi multirobot infrastructures," *IEEE Internet Things J.*, vol. 4, no. 6, pp. 2142–2158, Dec. 2017.
[30] A. Ebrahimzadeh and M. Maier, "Delay-constrained teleoperation task scheduling and assignment for human+machine hybrid activities over FiWi enhanced networks," *IEEE Trans. Netw. Service Manag.*, vol. 16, no. 4, pp. 1840–1854, Dec. 2019.
[31] S. Haddadin, L. Johannsmeier, and F. D. Ledezma, "Tactile robots as a central embodiment of the Tactile Internet," *Proc. IEEE*, vol. 107, no. 2, pp. 471–487, Feb. 2019.
[32] K. E. C. Booth, T. T. Tran, G. Nejat, and J. C. Beck, "Mixed-integer and constraint programming techniques for mobile robot task planning," *IEEE Robot. Autom. Lett.*, vol. 1, no. 1, pp. 500–507, Jan. 2016.
[33] J. A. Hernandez, R. Sanchez, I. Martin, and D. Larrabeiti, "Meeting the traffic requirements of residential users in the next decade with current FTTH standards: How much? How long?" *IEEE Commun. Mag.*, vol. 57, no. 6, pp. 120–125, Jun. 2019.
[34] S. Mondal, L. Ruan, and E. Wong, "Remote human-to-machine distance emulation through AI-enhanced servers for Tactile Internet applications," in *Proc. Opt. Netw. Commun. Conf. Exhibit. (OFC)*, Mar. 2020, pp. 1–3.
[35] Z. Kappassov, J.-A. Corrales, and V. Perdereau, "Tactile sensing in dexterous robot hands—Review," *Robot. Auton. Syst.*, vol. 74, pp. 195–220, 2015.
[36] (2019). *MANUS VR Virtual Reality Gloves*. [Online]. Available: https://manus-vr.com/
[37] K. Shoemake, "Animating rotation with quaternion curves," in *Proc. 12th Annu. Conf. Comput. Graph. Interact. Techn.*, 1985, pp. 245–254.
[38] I. F. Alves and C. Neves, *Extreme Value Distributions*. Heidelberg, Germany: Springer, 2011, pp. 493–496.
[39] K. Hornik, M. Stinchcombe, and H. White, "Multilayer feedforward networks are universal approximators," *Neural Netw.*, vol. 2, no. 5, pp. 359–366, Jul. 1989.
[40] M. A. Nielsen, *Neural Networks and Deep Learning*, vol. 2018. San Francisco, CA, USA: Determination Press, 2015.

[41] H. Liu, "On the Levenberg–Marquardt training method for feed-forward neural networks," in *Proc. 6th Int. Conf. Nat. Comput.*, vol. 1, Aug. 2010, pp. 456–460.
[42] K. S. Narendra and M. A. L. Thathachar, *Learning Automata: An Introduction*. Englewood Cliffs, NJ, USA: Prentice-Hall, 1989.
[43] S. Friston and A. Steed, "Measuring latency in virtual environments," *IEEE Trans. Vis. Comput. Graphics*, vol. 20, no. 4, pp. 616–625, Apr. 2014.
[44] H. Beyranvand, M. Lévesque, M. Maier, J. A. Salehi, C. Verikoukis, and D. Tipper, "Toward 5G: FiWi enhanced LTE-A HetNets with reliable low-latency fiber backhaul sharing and WiFi offloading," *IEEE/ACM Trans. Netw.*, vol. 25, no. 2, pp. 690–707, Apr. 2017.
[45] F. Palumbo, G. Aceto, A. Botta, D. Ciuonzo, V. Persico, and A. Pescape, "Characterizing cloud-to-user latency as perceived by AWS and Azure users spread over the globe," in *Proc. IEEE Global Commun. Conf. (GLOBECOM)*, 2019, pp. 1–6.

SOURAV MONDAL (Graduate Student Member, IEEE) received the B.Tech. degree in electronics and communication engineering from Kalyani Government Engineering College, West Bengal University of Technology and the M.Tech. degree in telecommunication systems engineering from the Department of Electronics and Electrical Communication Engineering, Indian Institute of Technology Kharagpur in 2012 and 2014, respectively. He is currently pursuing the Doctoral degree thesis with title "Strategic Deployment of Artificial Intelligence-Enhanced Cloudlets for Low-latency Human-to-Machine Applications" with the Department of Electrical and Electronic Engineering of the University of Melbourne.

LIHUA RUAN (Member, IEEE) received the M.S. degree from Northwestern Polytechnical University, Xi'an, China, in 2015, and the Ph.D. degree from the University of Melbourne, Melbourne, VIC, Australia, in 2019. Her current research interests include smart body area networks, wireless local area networks, and dynamic bandwidth resource allocation in passive optical networks, in conjunction with the use of machine learning techniques, for tactile Internet applications.

MARTIN MAIER (Senior Member, IEEE) received the M.Sc. and Ph.D. degrees (with Distinction) from the Technical University of Berlin, Germany, in 1998 and 2003, respectively. He is a Full Professor with the Institut National de la Recherche Scientifique, Montréal, Canada. In winter 2019 and 2020, he held a UC3M-Banco de Santander Excellence Chair with the Universidad Carlos III de Madrid, Madrid, Spain. He was a co-recipient of the 2009 IEEE Communications Society Best Tutorial Paper Award. In March 2017, he received the Friedrich Wilhelm Bessel Research Award from the Alexander von Humboldt Foundation in recognition of his accomplishments in research on FiWi enhanced mobile networks. In May 2017, he was named one of the three most promising scientists in the category "Contribution to a Better Society" of the Marie Skłodowska-Curie Actions in 2017 Prize Award of the European Commission. He was a Marie Curie IIF Fellow of the European Commission from March 2014 to February 2015.

DAVID LARRABEITI (Senior Member, IEEE) received the M.Sc. and Ph.D. degrees in telecommunications engineering from the University Politecnica de Madrid in 1991 and 1996, respectively. He is a Full Professor of switching and networking architectures with UC3M. From 1998 to 2006, he was an Associate Professor with UC3M and led a number of international research projects, where he is responsible for the e-Photon/ONe+ network of excellence on Optical Networking. His research interests include the design of the future Internet infrastructure, ultra-broadband multimedia transport, and traffic engineering over IP-MPLS backbones.

GOUTAM DAS (Member, IEEE) received the M.Tech. degree from the Indian Institute of Technology Kharagpur, Kharagpur, India, in 2001, and the Ph.D. degree from the University of Melbourne, Australia, in 2008. He has also worked as a Senior Research Engineer with General Electric Research and Development Center for 3.5 years from 2001 to 2004. He has also worked as a Postdoctoral Fellow with Ghent University, Belgium, from 2009 to 2011. He is currently working as an Assistant Professor with the Indian Institute of Technology Kharagpur. His research interest is in the area of both optical as well as wireless networking.

ELAINE WONG (Senior Member, IEEE) received the B.E. and Ph.D. degrees from the University of Melbourne, Melbourne, VIC, Australia, where she is currently a Professor. She has coauthored more than 150 journal and conference publications. Her research interests include energy-efficient optical and wireless networks, optical-wireless integration, broadband applications of vertical-cavity surface-emitting lasers, wireless sensor body area networks, and emerging optical, and wireless technologies for tactile Internet. She has served on the editorial board of the *Journal of Lightwave Technology* and the *Journal of Optical Communications and Networking*.